A quantitative study of network robustness in resting state fMRI in young and elder conditions

Jaime Gomez-Ramirez*[1], Yujie Li[2,4], Qiong Wu[3] and Jinglong Wu[5,3]

[1]*The Hospital for Sick Children, Department of Neuroscience and Mental Health, University of Toronto, Bay St. 686, Toronto, Canada*
[2]*Key Laboratory of Adolescent Cyberpsychology and Behavior (CCNU), Ministry of Education, Wuhan 430079, China*
[4] *School of Psychology, Central China Normal University, Wuhan 430079, China*
[3]*Biomedical Engineering Laboratory, Okayama University, 1-1-1 Tsushima-naka, Kita-ku, Okayama, Japan*
[5]*Intelligent Robotics Institute, School of Mechatronics Engineering,Beijing Institute of Technology, Beijing, China*

Abstract

Brain connectivity analysis have shown great promise in understanding of how aging affects functional connectivity, however, an explanatory framework to study healthy aging in terms of network efficiency is still missing. Here we study network robustness i.e., resilience to perturbations, in resting state functional connectivity networks (rs-fMRI) in young and elder subjects. We apply analytic measures of network communication efficiency in the human brain to make reasonable guesses about compensatory mechanisms elicited in aging. Specifically, we quantify the effect of "lesioning" (node cancelling) of either single regions-of-interest (ROI) or whole networks on global connectivity metrics (i.e., efficiency). We find that young

*Corresponding author jaime.gomez-ramirez@sickkids.ca

individuals are more resilient than old ones to random "lesioning" of brain areas, global network efficiency is over 3 times lower in older subjects relative to younger subjects. On the other hand, the "lesioning" of central and limbic structures in young subjects yield a larger efficiency loss than in older individuals. Overall our study shows a more idiosyncratic response to specific brain network "lesioning" in elder compared to young subjects, and that young adults are more resilient to random deletion of single nodes compared to old adults.

1 Introduction

It has been suggested that fluctuations in the BOLD[1] signal measured in humans in resting state represent the neuronal activity baseline and shape spatially consistent patterns [46], [26]. The slow fluctuations in the BOLD signal found in resting subjects are highly coherent within either structural or functional networks in the human brain. Functional correlation based on the synchrony of low-frequency blood flow fluctuations in resting state have been identified in the sensorimotor [37], visual [17], language [31], auditory [33] and attention [24] and the frontoparietal control system [57].

The visual identification of the overall connectivity patterns in resting state functional magnetic resonance imaging (rs-fMRI), has been assessed first and foremost using both model-based and model-free approaches. The former, uses voxel-wise analysis of brain images to build statistical parametric maps of brain activation [6]. While this approach has been successful in, for instance, the identification of motor networks [47], it shows important limitations when the seed voxel cannot be easily identified [41]. For example, in brain areas with unclear boundaries i.e., cognitive networks involved in memory or self processing operations [22]. Independent Component Analysis (ICA), on the other hand, is a model-free approach that allows separating resting fluctuations from other signal variations, resulting in a collection of spatial maps, one for each independent component, that represent functionally relevant networks in the brain [11]. While ICA has the advantage over the parametric approach that it does not need to assume a specific temporal model of correlation between regions of interest, the functional relevance of the different components is, however, computed relative to their resemblance to a number of networks, based on criteria that are not easily formalized [7].

A third approach, complementary to the other two that is becoming of paramount importance is the network-based approach. Graph-based techniques provide new insights into the structure-function relationship in the

[1]Blood-oxygen-level dependent contrast imaging is the method used in functional magnetic resonance imaging (fMRI) to determine which parts of the brain are most active.

healthy brain, aging and neuropathological disorders [20], [58], [32], [59], [62], [8], [48]. The use of graph theoretic techniques to model brain networks has shifted the emphasis from the identification of local subnetworks -default mode network, primary sensory motor network etc.- to the quantitative study of the topological and informational characteristics of large-scale brain networks. The quantitative analysis of complex networks have been rapidly adopted in the cognitive neuroscience community, linking graph theoretic metrics to brain network organization [9], [51], specific behavioral abnormalities [54], [13] and clinical outcomes [63], [2], [19] . It is of note that notable proponents of a modularist vision of brain connectivity to understand cognition, such as Gazzaniga [28], [27], has now embraced a "complex brain networks approach" [4].

Network-based approaches to rs-fMRI have demonstrated non-trivial topological properties of functional networks in the human brain. Large-scale anatomical connectivity analysis in the mammalian brain, shows that brain topology is neither random nor regular. Instead, small world architectures - highly clustered nodes connected thorough relatively short paths- have been identified in both structural and functional brain networks [60], [3].

Small world network properties have also been consistently found across different conditions, including normal development, aging, and in various pathological conditions [58], [1], [52]. While network-based studies have been successful in delineating generic network properties such as path length or clustering, additional work is needed in order to come to grips with the internal working of the systems. Computational simulations of disruptions in the network architecture of resting state can give clues about normal development and pathological conditions. For example, Supekar and colleagues [53] have shown that the deterioration of small world properties such as the lowering of the cluster coefficient, affect local network connectivity which in turn may work as a network biomarker for Alzheimer's disease. Abnormalities in small-worldness may also have a significant positive correlation in, for example, schizophrenia [40] and epilepsy [39], [64].

Transport network efficiency measures have been used to study the relationship between structural and resting state functional connectivity [30]. The effects of lesioning in white matter connections can be studied via the simulation of the removal of individual connections from the connectome. Irimia and Van Hornreport [34] using this technique, have been able to delineate "a core scaffold" or white matter network connections that when disrupted, trigger dramatic changes in the overall organization of the human connectome. However, a systematic study of the effects of simulated lesioning in rs-fMRI is still missing. In this paper we try to fill this gap, providing efficiency and robustness measures to quantify the impact of simulated lesioning.

Aging is a complex physiological process with multiple temporal and

spatial scales and it is unrealistic to expect any all encompasing predictive model of aging. Nevertheless, a common finding is that older subjects present reduced functional connectivity compared to young adults. We will try to replicate this finding and go beyond, identifying the brain networks that when disconnected from the rest, result in dramatic/mild efficiency loss in transmitting information.

Previous studies have shown that modularity in both young and elderly condition is not random [42], [50]. Nevertheless, a general picture of how normal aging affects network efficiency is missing. Here, we explore the hypothesis that normal aging is associated with changes in network efficiency. We investigate the hemispheric asymmetry reduction hypothesis [10], studying the effects of lesioning hemispheres separately in older compared to young adults.

The rest of the paper is structured as follows. Section 2 introduces the methodology followed in the data acquisition and reconstruction, data preprocessing, and data connectivity analysis in the young and elder conditions. Then, we build a model to study quantitatively how network robustness is affected upon the removal of either nodes and specific networks as well as edges in both conditions. The simulations of the model are shown in Section 3. The empirical and clinical implications of the model are discussed in Section 4.

2 Materials and Methods

2.1 Data acquisition

Forty-two healthy volunteers separated in two groups, twenty-three healthy young volunteers (ages 21-32; mean 22.7; male/female 23/0) and 19 healthy older volunteers (ages 60-78; mean 66.5; male/female 16/3; MMSE score 29.5 +- 0.1) took part in the fMRI experiment. All subjects had normal or corrected-to-normal vision and all the participants in both conditions have not been diagnosed with mild cognitive impairment nor psychiatric or neurological disorders. The study was approved by the ethics committee of Okayama University, and written informed consent was obtained before the study. All subjects were imaged using a 1.5 T Philips scanner vision whole-body MRI system (Okayama University Hospital, Okayama, Japan), which was equipped with a head coil. Functional MR images were acquired during rest when subjects were instructed to keep their eyes closed and not to think of anything in particular. The imaging area consisted of 32 functional gradient-echo planar imaging (EPI) axial slices (voxel size = 3x3x4mm^3, TR = 3000ms, TE = 50ms, FA = 90°, acquisition matrix = 80x79, FOV = 240x240mm^2, slice thickness=4mm, gap=0.5mm) that were used to obtain T2*-weighted fMRI images in the axial plane. We obtained 176 functional

volumes and excluded the first 4 scans from analysis. After the EPI scan, a T1-weighted 3D magnetization-prepared rapid acquisition gradient echo (MP-RAGE) sequence was acquired (TR = 9.4ms, TE = 4.6ms, FA=10°, acquisition matrix= 240x240, voxel size = 1x1x1mm^3, 200 contiguous axial slices).

2.2 Data preprocessing

Data were preprocessed using Statistical Parametric Mapping software SPM8 [2] and REST v1.7 [3]. To correct for differences in slice acquisition time, all images were synchronized to the middle slice. Subsequently, images were spatially realigned to the first volume due to head motion. None of the subjects in both conditions had head movements exceeding 2.5mm on any axis or rotations greater than 2.5°. After the correction, the imaging data were normalized to the Montreal Neurological Institute (MNI) EPI template supplied with SPM8 (resampled to 2x2x2mm^3 voxels) [4]. In order to avoid introducing artificially local spatial correlation, the normalized images were not smoothed. Finally, the resulting data were temporally band-pass filtered (0.01-0.08 Hz) to reduce the effects of low-frequency drifts and high-frequency physiological noises [35].

2.3 Anatomical parcellation

Before whole brain parcellation, several sources of spurious variance including the estimated head motion parameters, the global brain signal and the average time series in the cerebrospinal fluid and white matter regions were removed from the data through linear regression. It ought to be noted that Murphy and colleagues in [43] have pointed out that global signal removal may artificially introduce anti-correlated networks. The effect of the removal of the global signal on resting state correlation maps have been examined by Fox and colleagues [25], reaching to the conclusion that several characteristics of anticorrelated networks are not attributable to global signal removal and therefore suggesting a biological basis for those anticorrelations.

The fMRI data were parcellated into 90 regions using the automated anatomical labeling template (AAL) [55]. For each subject, the mean time series of each region was obtained by simply averaging the time series of all voxels within that region.

[2] http://www.fil.ion.ucl.ac.uk/spm/

[3] http://restfmri.net/forum/index.php

[4] http://imaging.mrc-cbu.cam.ac.uk/imaging/Templates

2.4 Brain network construction

To measure the functional connectivity among regions, we calculated the Pearson correlation coefficients between any possible pair of regional time series, and then obtained a temporal correlation matrix $(90x90)$ for each subject. We applied Fisher's r-to-z transformation to improve the normality of the correlation matrix. Then, two-tailed one-sample t-tests were performed for all the possible $4005 = \frac{90x89}{2}$ pairwise correlations across subjects to examine whether each inter-regional correlation significantly differed from zero. A Bonferroni-Holm correction for multiple comparisons was further used to threshold the correlation matrix into the adjacency matrix M shown in Figure 1. Finally, an undirected binary graph was acquired in which nodes represent brain regions and edges represent links between regions.

2.5 Information Efficiency

A quantitative understanding of network robustness, that is, functional network invariance under perturbation, can shed light on the properties that mediate in developmental, aging and pathological processes in the human brain. In essence, robustness measures the capacity of the network to perform the same function before and after a perturbation. Perturbations are events, internal or external, that elicit a change in the network configuration. Possible perturbations are the obliteration of one or more nodes and changes in the connectivity between nodes.

The efficiency of a network is a network centrality measure that quantifies the network's reliability in transmitting information. Latora and Marchiori [38] proposed a measure of network efficiency defined as the efficiency in transmitting information between any two nodes (i, j) in a graph G as the inverse of the shortest path that connects them

$$\varepsilon_{ij} = \frac{1}{d_{ij}} \tag{1}$$

where d_{ij} is the shortest path length or the geodesic distance between nodes i and j. Note that when there is no path that connects the nodes i and j, $d_{ij} = \infty$, and the efficiency in the communication of the two nodes is zero, $\varepsilon_{ij} = 0$.

The efficiency of the network G, $\Sigma(G)$, is then calculated as the average of the efficiency between any two nodes ε_{ij}

$$\Sigma(G) = \frac{\sum_{i \neq j} \varepsilon_{ij}}{N(N-1)} = \frac{1}{N(N-1)} \frac{1}{\sum_{i \neq j} d_{ij}} \tag{2}$$

where N is the number of nodes.

We can calculate the *information centrality* C of any node i in a network G as the variation in the network efficiency caused by the removal of the

edges incident in i. Thus, the information centrality of a node i, C_i, is the difference between the efficiency of the original network G with N nodes and E edges, $G(N,E)$, and the efficiency of the resulting graph $G(N-i,E-k_i)$ with $N-i$ nodes and $E-k_i$ edges, where k_i denotes the set of edges incident to node i. The centrality of a node is a normalized measure of the loss in network efficiency, caused by the isolation of a node in G. Thus, the centrality of node i or the *efficiency loss* after the disconnection of node i is

$$C_i = \frac{\Sigma(G(N,E)) - \Sigma(G(N-i,E-k_i))}{\Sigma(G(N,E))} \tag{3}$$

From equation 3, a network G is considered to be robust to a perturbation if the network efficiency, $\Sigma(G)$, stays close to the original value after a perturbation. Ideally, $\Sigma(G(N,E)) = \Sigma(G(N-i,E-k_i))$ with efficiency loss or centrality of node i equals to 0.

By the same token, the information centrality of a set of nodes S or the efficiency loss upon the removal of S, can be calculated as the normalized measure of the loss in network efficiency caused by the isolation of a set of nodes S in G.

$$C_S = \frac{\Sigma(G(N,E)) - \Sigma(G(N-S,E-k_S))}{\Sigma(G(N,E))} \tag{4}$$

3 Results

The global network efficiency for unperturbed networks as defined in equation 2 is 0.3678 for young subjects and 0.1144 for elder subjects. Thus, young subjects connectivity network is slightly more than three times more efficient in terms of the shortest path distance between any two nodes as calculated in equation 2.

In order to obtain the efficiency measures described in equations 3 and 4, we perturb the resting state network in three ways. First, using random single node deletion (Section 3.1), second targeting specific networks of interest (Section 3.2) and third the efficiency loss after lesioning edges (Section 3.3).

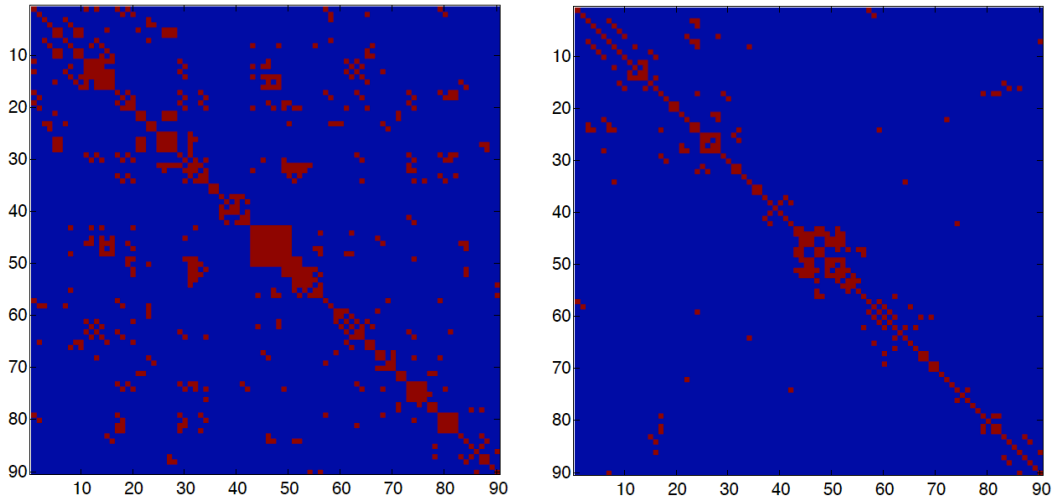

Figure 1: (a) Adjacency matrix in the young condition. (b) Adjacency matrix old condition. The adjacency matrix $M(i,j) = 1$ if there is a significant correlation between brain regions i and j and $M(i,j) = 0$, otherwise The red dots represent connections between two nodes. The number of edges in the young condition is 718 and in the young condition is 308, the average degree connectivity is 8.97 and 4.42, respectively.

3.1 Efficiency after single node lesioning

Here we build a population of networks created by the systematic lesioning of single nodes. The population of perturbations P that result from the systematic deletion of all nodes in all possible combinations has as many networks as

$$|P| = \sum_{i=1}^{N} C(N,i) = \frac{N!}{(i!)(N-i)!}$$

For example, the population of networks that result from the deletion of one single node has 90 networks

$$\sum_{i=1}^{1} C(90,i) = \frac{90!}{(1!)(90-1)!} = 90$$

Similarly, the number of perturbed networks obtained by deleting two nodes in all possible ways contains 4005 networks

$$\sum_{i=1}^{2} C(90,i) = \frac{90!}{(2!)(90-2)!} = 4005$$

We build a distribution of the efficiency measures described in section 2 for both young and elder condition for the systematic removal of one node.

Thus, in the young condition, we denote $P_{y,90}$ the distribution of networks with only one node removed, that is, $P_{y,90}$ has 90 different networks where for each of of them, one node and its connections have been deleted. The mean of the efficiency measure for $P_{y,90}$ is 0.358. The most significant loss in efficiency occurs with the removal of node 74 ("Lenticular nucleus, putamen") followed by node 31 ("Insula right") . The average efficiency loss in the young condition is 2.44"%" with a maximum of 4.67"%" for node 74 ("Lenticular nucleus, putamen") and no efficiency loss for node 89 ("temporal pole: middle temporal gyrus") (Figure 2). The rationale for the different impact in the efficiency caused by the obliteration of certain nodes can be found in the connectivity degree. In general, the nodes that after their removal trigger a low efficiency loss have also low connectivity degree, and those that produce a more pronounced reduction of the network efficiency tend to be more connected (Figure 3, Figure 4).

Similarly, for the elder condition, we denote $P_{e,90}$ the distribution of networks with only one node removed. The mean of the efficiency measure (equation 2) for the 90 networks obtained upon single node deletion is 0.109. As it happened in the young condition, the removal of node 89 ("Temporal pole: middle temporal gyrus") has no effect in the efficiency. Interestingly, the removal of nodes with the lowest connectivity degree (2) have also no quantifiable effect in the network efficiency (Figure 2).

The most significant loss in efficiency occurs with the removal of node node 62 ("Inferior parietal, but supramarginal and angular gyri"). After the removal of this node, the efficiency loss relative to the original network is the 32.87"%". This is an interesting result since node 62 is not a highly connected node, its connectivity degree is 6. Nodes 24 ("Superior frontal gyrus, medial"), 44 ("Calcarine fissure and surrounding cortex") and 51 ("Middle occipital gyrus") have more connections, connectivity degree 10, and upon their deletion the efficiency loss is not as severe as in the case of node 62. The mean efficiency loss in the elder condition after the removal of a single node is 4.61"%" (in the young condition is 2.44"%").

The connectivity degree alone is a much worse predictor of efficiency loss for old than for young subjects (Figure 3 and Figure 4). This is in agreement with the literature of functional connectivity in healthy aging. The process of aging underlies global reorganization of brain functional networks that reflect the topological changes observed across the human lifespan [12], [50]. Furthermore, as shown in [29] brain networks in the elderly showed decreased modularity (less distinct functional networks) and decreased local efficiency.

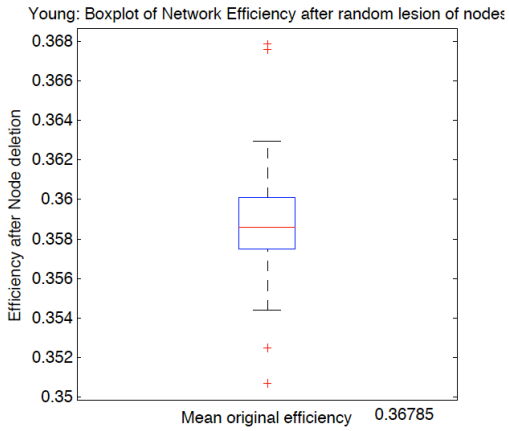

(a) Young: Network efficiency after one node deletion

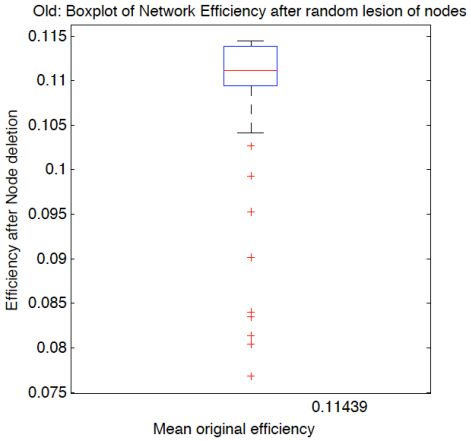

(b) Old: Network efficiency after one node deletion

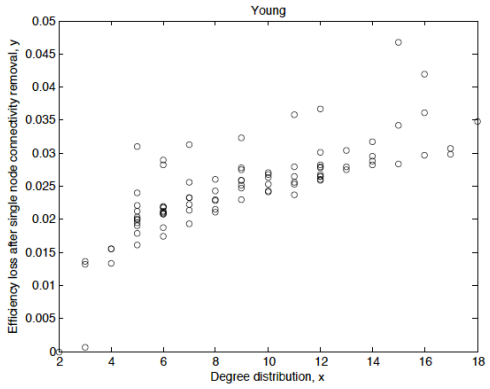

(c) Young: Degree distribution (X) Efficiency loss (Y)

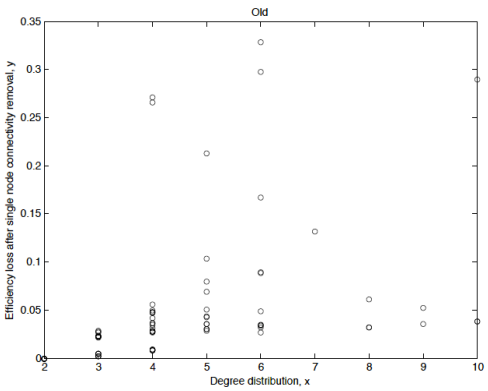

(d) Old: Degree distribution (X) Efficiency loss (Y)

Figure 2: (a) Boxplot of network efficiency after random lesion of individual nodes in young subjects. Only a very few nodes fall outside the box whose edges are the 25th and 75th percentiles. (b) Boxplot of network efficiency after random lesion of individual nodes in old subjects. More nodes fall outside below the 25th percentile than in the young condition. The distribution in the elder condition is more skewed than in the young condition.(c) Degree distribution (x-axis) and efficiency loss or node centrality (y-axis) after single node connectivity removal in the young condition. (d) Degree distribution (x-axis) and efficiency loss node centrality (y-axis) after single node connectivity removal in the elder condition. Each dot in charts (c) and (d) represents a node with connectivity degree equals to x that upon its removal produces a variation in the network efficiency equals to y, normalized between 0 (no efficiency loss) and 1 (maximum efficiency loss). The linear regression in the young condition is 0.755 and in the old condition is 0.4002.

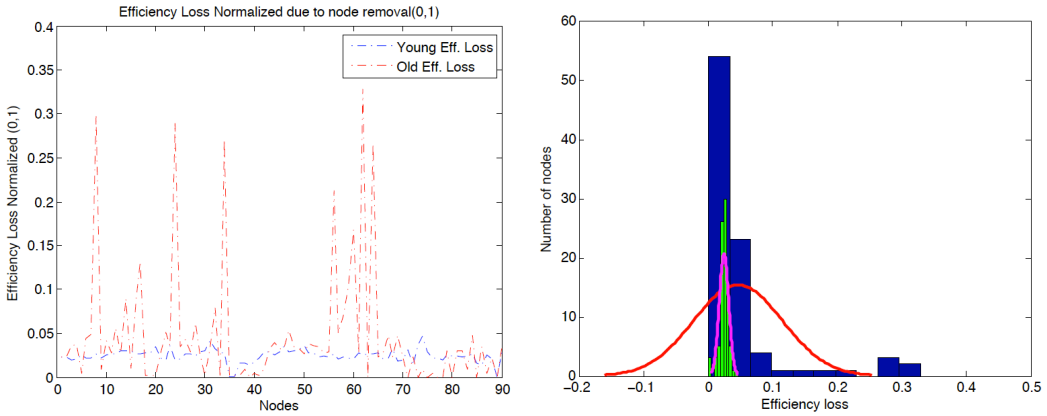

(a) Efficiency loss in young (blue) and old (red) for single node removal

(b) Frequency bars for efficiency loss in young (green) and old (blue) for single node removal

Figure 3: (a) Efficiency loss normalized (0,1) due to the removal of single nodes in both conditions. While in the young condition there are no nodes that upon its removal the efficiency of the resulting network deteriorates drastically, in the elder condition, there are 6 nodes that upon their removal trigger a 20% or more reduction in the network efficiency. The efficiency loss of node 8 ("Middle frontal gyrus"), 29.7%, node 24 ("Superior frontal gyrus, medial"), 28.9%, node 34 ("Median cingulate and paracingulate gyri"), 27.1%, node 56 ("Fusiform gyrus"),21.2%, node 62 ("Inferior parietal, but supramarginal and angular gyri"), 32.8% and node 64 ("Supramarginal gyrus"), 26.5%. (b) Distribution of efficiency loss after node removal in both young (green histogram) and elder condition (blue histogram). The efficiency loss in the young condition is narrow. The elder condition, on the other hand, has a more spread distribution of efficiency values. The spread or difference between maximum and minimum efficiency loss in efficiency loss among nodes is 4.67% for young subjects and 32.87% for old subjects.

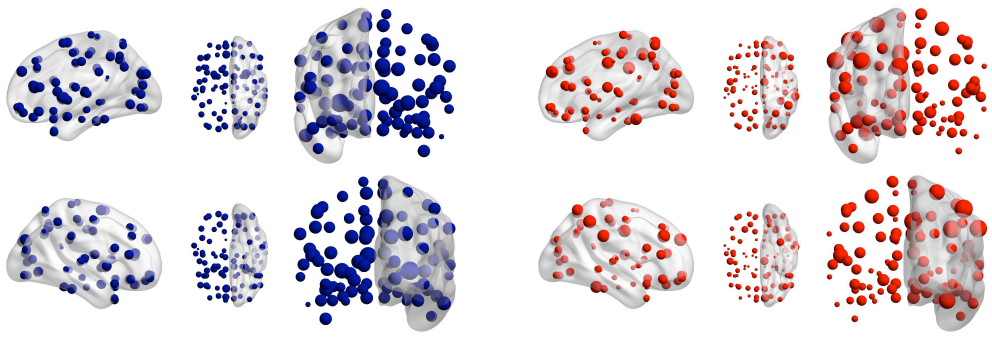

(a) Efficiency loss in young subjects

(b) Efficiency loss in old subjects

Figure 4: Efficiency loss in young and elder condition for single node removal. The larger the dot size, the larger is the efficiency loss upon its removal.

3.2 Efficiency after target networks lesioning

So far, we have quantified the efficiency loss due to the removal of single nodes, in this section we investigate how the efficiency measure is affected by the removal of entire networks of interest. In particular, we study the efficiency loss of the Default Mode Network (DMN), temporal lobe, frontal lobe, insula and cingulate gyrus, occipital lobe, parietal lobe, central structures and limbic structures. The numerical results are displayed in table 1 and brain connectivity is shown in figure 5).

The DMN is commonly considered to consist of medial prefrontal cortex (AAL 23, 24, 25, 26), posterior cingulate cortex/precuneus (AAL 35, 36/67 68) and bilateral inferior parietal lobule (AAL 61, 62). The removal of the DMN in young adults triggers an efficiency loss of the 19.6%. In the elder condition, the same procedure yields an efficiency reduction of 61.66%. It is remarkable that in the elder condition the lesioning of the DMN network, which represents the 11% of the total regions 90 regions, bring down the efficiency of the network to 61.66%. The strong efficiency reduction associated with the lesioning of the DMN in old subjects is coherent with the hypothesis that there is a decrease in activity in the DMN in aging [36]. This age-based reduction in DMN activity can trigger mechanisms that compensate the loss in DMN activity with an increase in connectivity between the DMN and other networks [16]. According to this hypothesis, the DMN becomes a more central network and upon the lesioning of the DMN a dramatic efficiency loss is produced.

The removal of the frontal lobe, the parietal lobe and the temporal lobe have as well a larger impact in the elder condition than in the young condition. Interestingly, we have identified three brain structures in which the lesioning in young individuals has a larger impact compared to old subjects. The lesioning of the occipital lobe trigger a slightly lower efficiency loss value in the old condition compared to the young condition. More interestingly is the lesioning of the limbic structures and the central structures. The efficiency loss for these structures shows a distinct difference between young and old individuals with larger values for the former. The minor impact of the lesioning of central and limbic structures in the old condition is conforming with the literature that shows degradation of fronto-stratial network in aging [49] and the break-down between the hipocampal regions and the DMN [23].

3.3 Efficiency after target networks lesioning of edges

To test the hypothesis that that the relationship between the hippocampus and the DMN tends to break down with age, we need to lesion the edges that connect these brain structures rather than nodes as we have done in the previous sections. Salami et al. show that [49] elevated hippocampal activity

Target Brain Structure	AAL regions	Eff.loss Young	Eff.loss Old
DMN	3 24 25 26 35 36 37 68 61 62	19.66%	61.66%
Frontal Lobe	1 2 3 4 5 6 7 8 9 10 11 12 13 14 15 16 17 18 51 52	42.83%	67.07%
Temporal Lobe	37 38 39 40 41 42 55 56 79 80 81 82 83 84 85 86 87 88 89 90	33.56%	41%
Occipital Lobe	43 44 45 46 47 48 49 50 51 52 53 54	31.71%	30.79%
Parietal Lobe	57 58 59 60 61 62 63 64 65 66 67 68	26.65%	45.64%
Insula and cingulate gyrus	3 24 25 26 35 36 37 68 61 62	18.72%	36.91%
Central structures (Caudate nucleus, putamen, pallidum, thalamus)	71 72 73 74 75 76 77 78	23.01%	3.16%
Limbic structures (hippocampus, parahippocampus, amygdala)	37 38 39 40 41 42	9.30%	1.40%

Table 1: The table shows the efficiency loss after the disconnection of different brain structures in both conditions. Interestingly, the reduction in efficiency is not always more pronounced in the elder condition. For example, the disconnection of the central structures (caudate nucleus, putamen, pallidum and thalamus) triggers a larger efficiency disruption in young than in old individuals. A similar situation, larger efficiency loss in young compared old condition, also occurs with the disconnection of the limbic structures (hippocampus, parahippocampus and amygdala) and the occipital lobe areas. The table shows the efficiency loss in both young and old condition when target networks are lesioned. The lesion consists on the obliteration of the nodes defined in the second column. The efficiency loss is larger in old adults with the exception of the occipital lobe, the central structures and the limbic structures. The reduction of efficiency in the central structures is particularly interesting since in the old condition it yields only a 3.16% reduction in efficiency while in the young condition the efficiency loss for the same lesioning yields a reduction of 23.01%.

at rest may lower the degree to which the hippocampus interacts with other regions during memory tasks, and thus results in memory deficits. However, this view is not uncontested and in [15] it is suggested that connectivity between left and right hippocampus is negatively related to age. In our study the efficiency loss produced by the disconnection of the left and the right side of hippocampal and parahippocampal areas does not yield a reduction of efficiency loss since these areas are not connected in the old subjects (Table 2).

We test the asymmetry hypothesis by which brain activity shows a more balance activity among the two hemispheres with age, that is, the hypothesis predicts that in young individuals, brain activity is more asymmetric than in old individuals. The asymmetry hypothesis summons that in young individuals the difference in efficiency loss for disconnecting the two hemispheres is expected to be larger than in the old condition. The rationale behind the hypothesis is that during aging the brain tries to compensate the reduction of activity level, for example in the DMN, by balancing activity across the brain. In young adults, we find that if one of the two hemispheres is entirely lesioned (all areas of one hemisphere are unreacheable from the opposed hemisphere) the efficiency loss is very similar. Precisely, the efficiency loss when the left side is lesioned is 75.32% and when the lesioning occurs in the right side the efficiency loss is 77.01%. In old subjects, the lesioining of the right side has a more pronounced impact in the efficiency loss, 91.21% for the removal of the right side and 70.89% for the removal of the left side. This result is consistent with the HAROLD (hemispheric asymmetry reduction in older adults) model proposed by Cabeza [10]. The difference in efficiency loss in old subjects after entire hemispheral disconnection is 10 times larger ($\sim 20\%$) than in the young subjects ($\sim 2\%$) indicates that old subjects are more sensitive or less robust to unilateral disruptions because aging process tend to reduce hemispheric asymmetry. Based on this results, we hypothesize that a process of de-differentiation may be a key mechanism to explain age-related hemispheric asymmetry reductions. As it was already mentioned in section 3.1 the efficiency loss triggered by the disconnection of brain areas is more stereotypical (less differentiated) in the elder condition than in young condition.

4 Discussion

The objective of this work is to study network robustness i.e., resilience to perturbations, in resting state functional connectivity networks in young and elderly conditions. The literature reviewed here suggests that graph-based network analyses are capable of uncovering system-level changes associated with aging in the resting brain. We have analyzed the functional connectivity in resting state using a perturbational approach consisting on either the

Table 2: Efficiency loss caused by the deletion of edges that connect brain regions in young and elder conditions. For example DMN-DMN is the deletion of the edges that connect the right and the side of the DMN, DMN-HC the edges that connect DMN and HC, including parahippocampal areas

Network-Network Edges disconnection	Eff.loss Young	Eff.loss Old
DMN-DMN	0.64%	0.99%
HC-HC	1.43%	0.45%
HC-DMN	0.16%	0%
Frontal-Stratium	0.37%	0%

systematic removal of single nodes and the removal of entire networks of interest such as the DMN and others, and we have computed the loss in network efficiency.

Our results expand previous works on the study of robustness of structural brain networks. Interestingly, we find that the distribution of network efficiency in the young and the elder condition show very different signatures. This is consistent with existing evidence [42] that both young and elderly conditions show non random modularity and that normal aging brain is associated with changes in modularity [50].

The efficiency loss in young subjects, upon the removal of single nodes is always below the 5%, while in the elder condition the removal of individual nodes may yield a dramatic reduction of the network efficiency (maximum of 32.87%). The young adults are, thus, more robust to random deletion of single nodes. However, when the lesioning is focused in specific brain networks rather than single regions, the efficiency loss for young subjects is in occassions higher than when the same damage is done in old subjects. For example, the disconnection of the occipital lobe, limbic structures and central structures yield larger efficiency loss in the young condition. This result is compatible with previous studies in normal healthy aging that show an increase in functional connectivity in the sensorimotor network and a decrease in resting state networks, including the DMN [50]. The continuum decrease in DMN functional connectivity found from normal aging to mild cognitive impairment and to Alzheimer's disease (AD) can be quantitatively studied. The lowering of DMN activity is associated with better performance on attention-demanding tasks, and DMN hyperactivity is being related to negative rumination and depression [61].

We replicate the common finding that older subjects present reduced functional connectivity compared to young adults [48]. Healthy normal ag-

ing is associated with cognitive decline and the functional disconnection observed here and other studies might play an important role [21], [18]. We observe largest values of efficiency loss in old adults compared to young adults in the Default-Mode-Network and the frontal lobe (Table 1). This is consistent with the compensation hypothesis in healthy aging which states that older adults brains compensate for the overall functional deficits by increasing the activity levels in frontal regions, as part of a reorganization process mediated by healthy normal aging [10], [45]. In this view, the DMN is a highly susceptible system in healthy aging [5], [44].

Can efficiency loss be used as a predictor of brain network differential activity? Vergun et al. [56] applied a Support Vector Machine (SVM) linear classifier to rs-fMRI data in order to compare age-related differences in four of the major functional brain networks: the default, cingulo-opercular, fronto-parietal, and sensorimotor. The classifier was able to detect "connectivity hubs", or nodes with the most significant features that influenced age classification. More work is however needed in order to properly address the compatibility of informational efficiency measures with non parametric classifiers.

A natural continuation of this work is to incorporate a translational outlook to, for example, investigate whether hubs of human brain networks are more likely to be anatomically abnormal than non-hubs in brain disorders [14]. Informational efficiency measures may also shed light on the dynamics and control of resting state networks in mental disorders. This perturbational approach can also be extended to study the interplay between network efficiency and brain metabolic demand, aiming to identify pathological signatures for early diagnosis in neurodegenerative disorders. The network dynamics associated with different conditions -normal healthy aging, mild cognitive impairment, Alzheimer's disease etc.- can be simulated with the same or similar type of functional intervention proposed here. Interventions other than disconnecting regions of interest or entire subnetworks from the whole brain, may include stress simulations induced by impairment of structural, functional or both connectivity patterns in multimodal imaging models. The computational lesioning of brain foci holds promise for systemic understanding of compensatory and other network mechanisms e.g., cascade and contagion effects, under normal and pathological conditions.

References

[1] A. Anderson and M. S. Cohen. Decreased small-world functional network connectivity and clustering across resting state networks in schizophrenia: an fMRI classification tutorial. *Frontiers in Human Neuroscience*, 7:520, 2013.

[2] J. S. Anderson, J. A. Nielsen, M. A. Ferguson, M. C. Burback, E. T. Cox, L. Dai, G. Gerig, J. O. Edgin, and J. R. Korenberg. Abnormal brain synchrony in Down Syndrome. *NeuroImage: Clinical*, 2:703–715, 2013.

[3] D. S. Bassett and E. Bullmore. Small-world brain networks. *The Neuroscientist*, 12(6):512–523, Dec. 2006.

[4] D. S. Bassett and M. S. Gazzaniga. Understanding complexity in the human brain. *Trends in cognitive sciences*, 15(5):200–209, May 2011. PMID: 21497128.

[5] R. F. Betzel, L. Byrge, Y. He, J. Goni, X.-N. Zuo, and O. Sporns. Changes in structural and functional connectivity among resting-state networks across the human lifespan. *NeuroImage*, 102 Pt 2:345–357, Nov. 2014.

[6] B. Biswal, F. Z. Yetkin, V. M. Haughton, and J. S. Hyde. Functional connectivity in the motor cortex of resting human brain using echo-planar MRI. *Magnetic resonance in medicine: official journal of the Society of Magnetic Resonance in Medicine / Society of Magnetic Resonance in Medicine*, 34(4):537–541, Oct. 1995. PMID: 8524021.

[7] B. B. Biswal, M. Mennes, X.-N. Zuo, S. Gohel, C. Kelly, S. M. Smith, C. F. Beckmann, J. S. Adelstein, R. L. Buckner, S. Colcombe, A.-M. Dogonowski, M. Ernst, D. Fair, M. Hampson, M. J. Hoptman, J. S. Hyde, V. J. Kiviniemi, R. KÃűtter, S.-J. Li, C.-P. Lin, M. J. Lowe, C. Mackay, D. J. Madden, K. H. Madsen, D. S. Margulies, H. S. Mayberg, K. McMahon, C. S. Monk, S. H. Mostofsky, B. J. Nagel, J. J. Pekar, S. J. Peltier, S. E. Petersen, V. Riedl, S. A. R. B. Rombouts, B. Rypma, B. L. Schlaggar, S. Schmidt, R. D. Seidler, G. J. Siegle, C. Sorg, G.-J. Teng, J. Veijola, A. Villringer, M. Walter, L. Wang, X.-C. Weng, S. Whitfield-Gabrieli, P. Williamson, C. Windischberger, Y.-F. Zang, H.-Y. Zhang, F. X. Castellanos, and M. P. Milham. Toward discovery science of human brain function. *Proceedings of the National Academy of Sciences of the United States of America*, 107(10):4734–4739, Mar. 2010.

[8] M. R. Brier, J. B. Thomas, A. M. Fagan, J. Hassenstab, D. M. Holtzman, T. L. Benzinger, J. C. Morris, and B. M. Ances. Functional connectivity and graph theory in preclinical Alzheimer's disease. *Neurobiology of Aging*, 35(4):757–768, Apr. 2014.

[9] E. Bullmore and O. Sporns. Complex brain networks: graph theoretical analysis of structural and functional systems. *Nature reviews. Neuroscience*, 10(3):186–198, Mar. 2009. PMID: 19190637.

[10] R. Cabeza, N. D. Anderson, J. K. Locantore, and A. R. McIntosh. Aging gracefully: compensatory brain activity in high-performing older adults. *NeuroImage*, 17(3):1394–1402, Nov. 2002.

[11] V. D. Calhoun, J. Liu, and T. Adali. A review of group ICA for fMRI data and ICA for joint inference of imaging, genetic, and ERP data. *NeuroImage*, 45(1 Suppl):S163–172, Mar. 2009.

[12] M. Cao, J.-H. Wang, Z.-J. Dai, X.-Y. Cao, L.-L. Jiang, F.-M. Fan, X.-W. Song, M.-R. Xia, N. Shu, Q. Dong, M. P. Milham, F. X. Castellanos, X.-N. Zuo, and Y. He. Topological organization of the human brain functional connectome across the lifespan. *Developmental Cognitive Neuroscience*, 7:76–93, Jan. 2014.

[13] L. Cocchi, B. J. Harrison, J. Pujol, I. H. Harding, A. Fornito, C. Pantelis, and M. Yacel. Functional alterations of large-scale brain networks related to cognitive control in obsessive-compulsive disorder. *Human Brain Mapping*, 33(5):1089–1106, May 2012.

[14] N. A. Crossley, A. Mechelli, J. Scott, F. Carletti, P. T. Fox, P. McGuire, and E. T. Bullmore. The hubs of the human connectome are generally implicated in the anatomy of brain disorders. *Brain*, 137(8):2382–2395, Aug. 2014.

[15] J. Damoiseaux, R. Viviano, P. Yuan, and N. Raz. Adult age differences in functional connectivity in the default mode network. In *Organization for Human Brain Mapping*, Hawaii,US, 2015.

[16] J. S. Damoiseaux, C. F. Beckmann, E. J. S. Arigita, F. Barkhof, P. Scheltens, C. J. Stam, S. M. Smith, and S. a. R. B. Rombouts. Reduced resting-state brain activity in the "default network" in normal aging. *Cerebral Cortex (New York, N.Y.: 1991)*, 18(8):1856–1864, Aug. 2008.

[17] J. S. Damoiseaux, S. A. R. B. Rombouts, F. Barkhof, P. Scheltens, C. J. Stam, S. M. Smith, and C. F. Beckmann. Consistent resting-state networks across healthy subjects. *Proceedings of the National Academy of Sciences of the United States of America*, 103(37):13848–13853, Sept. 2006. PMID: 16945915.

[18] E. L. Dennis and P. M. Thompson. Functional brain connectivity using fMRI in aging and Alzheimer's disease. *Neuropsychology Review*, 24(1):49–62, Mar. 2014.

[19] B. C. Dickerson and R. A. Sperling. Large-scale functional brain network abnormalities in AlzheimerâĂŹs disease: Insights from functional neuroimaging. *Behavioural neurology*, 21(1):63–75, 2009.

[20] D. A. Fair, A. L. Cohen, J. D. Power, N. U. F. Dosenbach, J. A. Church, F. M. Miezin, B. L. Schlaggar, and S. E. Petersen. Functional brain net-

works develop from a "local to distributed" organization. *PLoS computational biology*, 5(5):e1000381, May 2009.

[21] L. K. Ferreira and G. F. Busatto. Resting-state functional connectivity in normal brain aging. *Neuroscience and Biobehavioral Reviews*, 37(3):384–400, Mar. 2013.

[22] A. A. Fingelkurts and A. A. Fingelkurts. Persistent operational synchrony within brain default-mode network and self-processing operations in healthy subjects. *Brain and Cognition*, 75(2):79–90, Mar. 2011.

[23] A. M. Fjell, M. H. Sneve, A. B. Storsve, H. Grydeland, A. Yendiki, and K. B. Walhovd. Brain Events Underlying Episodic Memory Changes in Aging: A Longitudinal Investigation of Structural and Functional Connectivity. *Cerebral Cortex*, page bhv102, May 2015.

[24] M. D. Fox, M. Corbetta, A. Z. Snyder, J. L. Vincent, and M. E. Raichle. Spontaneous neuronal activity distinguishes human dorsal and ventral attention systems. *Proceedings of the National Academy of Sciences of the United States of America*, 103(26):10046–10051, June 2006. PMID: 16788060.

[25] M. D. Fox, D. Zhang, A. Z. Snyder, and M. E. Raichle. The Global Signal and Observed Anticorrelated Resting State Brain Networks. *Journal of Neurophysiology*, 101(6):3270–3283, June 2009.

[26] P. Fransson. How default is the default mode of brain function?: Further evidence from intrinsic BOLD signal fluctuations. *Neuropsychologia*, 44(14):2836–2845, 2006.

[27] J. Fuster. The module: crisis of a paradigm book review, "the new cognitive neurosciences" 2nd edition, m.s. gazzaniga, editor-in-chief, mit press. *Neuron*, (26):51–53, 2000.

[28] M. S. Gazzaniga, editor. *The New Cognitive Neurosciences: Second Edition*. The MIT Press, 2 edition, Nov. 1999.

[29] L. Geerligs, R. J. Renken, E. Saliasi, N. M. Maurits, and M. M. Lorist. A Brain-Wide Study of Age-Related Changes in Functional Connectivity. *Cerebral Cortex (New York, N.Y.: 1991)*, 25(7):1987–1999, July 2015.

[30] J. Goni, M. P. v. d. Heuvel, A. Avena-Koenigsberger, N. V. d. Mendizabal, R. F. Betzel, A. Griffa, P. Hagmann, B. Corominas-Murtra, J.-P. Thiran, and O. Sporns. Resting-brain functional connectivity predicted by analytic measures of network communication. *Proceedings of the National Academy of Sciences*, 111(2):833–838, Jan. 2014.

[31] M. Hampson, B. S. Peterson, P. Skudlarski, J. C. Gatenby, and J. C. Gore. Detection of functional connectivity using temporal correlations

in MR images. *Human brain mapping*, 15(4):247–262, Apr. 2002. PMID: 11835612.

[32] Y. He and A. Evans. Graph theoretical modeling of brain connectivity. *Current opinion in neurology*, 23(4):341–350, Aug. 2010. PMID: 20581686.

[33] M. D. Hunter, S. B. Eickhoff, T. W. R. Miller, T. F. D. Farrow, I. D. Wilkinson, and P. W. R. Woodruff. Neural activity in speech-sensitive auditory cortex during silence. *Proceedings of the National Academy of Sciences of the United States of America*, 103(1):189–194, Jan. 2006. PMID: 16371474.

[34] A. Irimia and J. D. Van Horn. Systematic network lesioning reveals the core white matter scaffold of the human brain. *Frontiers in Human Neuroscience*, 8:51, 2014.

[35] Q. Jiao, G. Lu, Z. Zhang, Y. Zhong, Z. Wang, Y. Guo, K. Li, M. Ding, and Y. Liu. Granger causal influence predicts BOLD activity levels in the default mode network. *Human Brain Mapping*, 32(1):154–161, Jan. 2011.

[36] W. Koch, S. Teipel, S. Mueller, K. Buerger, A. L. W. Bokde, H. Hampel, U. Coates, M. Reiser, and T. Meindl. Effects of aging on default mode network activity in resting state fMRI: does the method of analysis matter? *NeuroImage*, 51(1):280–287, May 2010.

[37] S.-M. Kokkonen, J. Nikkinen, J. Remes, J. Kantola, T. Starck, M. Haapea, J. Tuominen, O. Tervonen, and V. Kiviniemi. Preoperative localization of the sensorimotor area using independent component analysis of resting-state fMRI. *Magnetic resonance imaging*, 27(6):733–740, July 2009. PMID: 19110394.

[38] V. Latora and M. Marchiori. Efficient behavior of small-world networks. *Physical Review Letters*, 87(19):198701, Oct. 2001.

[39] W. Liao, Z. Zhang, Z. Pan, D. Mantini, J. Ding, X. Duan, C. Luo, G. Lu, and H. Chen. Altered functional connectivity and small-world in mesial temporal lobe epilepsy. *PLoS ONE*, 5(1):e8525, Jan. 2010.

[40] Y. Liu, M. Liang, Y. Zhou, Y. He, Y. Hao, M. Song, C. Yu, H. Liu, Z. Liu, and T. Jiang. Disrupted small-world networks in schizophrenia. *Brain: a journal of neurology*, 131(Pt 4):945–961, Apr. 2008. PMID: 18299296.

[41] J. A. Maldjian. Functional Connectivity MR Imaging: Fact or Artifact? *American Journal of Neuroradiology*, 22(2):239–240, Feb. 2001.

[42] D. Meunier, S. Achard, A. Morcom, and E. Bullmore. Age-related changes in modular organization of human brain functional networks. *NeuroImage*, 44(3):715–723, Feb. 2009.

[43] K. Murphy, R. M. Birn, D. A. Handwerker, T. B. Jones, and P. A. Bandettini. The impact of global signal regression on resting state correlations: are anti-correlated networks introduced? *NeuroImage*, 44(3):893–905, Feb. 2009.

[44] K. Onoda, M. Ishihara, and S. Yamaguchi. Decreased Functional Connectivity by Aging Is Associated with Cognitive Decline. *Journal of Cognitive Neuroscience*, 24(11):2186–2198, July 2012.

[45] D. C. Park and P. Reuter-Lorenz. The adaptive brain: aging and neurocognitive scaffolding. *Annual Review of Psychology*, 60:173–196, 2009.

[46] M. E. Raichle and D. A. Gusnard. Intrinsic brain activity sets the stage for expression of motivated behavior. *The Journal of Comparative Neurology*, 493(1):167–176, 2005.

[47] S. Robinson, G. Basso, N. Soldati, U. Sailer, J. Jovicich, L. Bruzzone, I. Kryspin-Exner, H. Bauer, and E. Moser. A resting state network in the motor control circuit of the basal ganglia. *BMC Neuroscience*, 10(1):137, Nov. 2009.

[48] R. Sala-Llonch, C. Junque, E. M. Arenaza-Urquijo, D. Vidal-Pineiro, C. Valls-Pedret, E. M. Palacios, S. Domenech, A. Salva, N. Bargallo, and D. Bartres-Faz. Changes in whole-brain functional networks and memory performance in aging. *Neurobiology of Aging*, 35(10):2193–2202, Oct. 2014.

[49] A. Salami, S. Pudas, and L. Nyberg. Elevated hippocampal resting-state connectivity underlies deficient neurocognitive function in aging. *Proceedings of the National Academy of Sciences*, 111(49):17654–17659, Dec. 2014.

[50] J. Song, R. M. Birn, M. Boly, T. B. Meier, V. A. Nair, M. E. Meyerand, and V. Prabhakaran. Age-related reorganizational changes in modularity and functional connectivity of human brain networks. *Brain Connectivity*, 4(9):662–676, Nov. 2014.

[51] O. Sporns. Contributions and challenges for network models in cognitive neuroscience. *Nature Neuroscience*, 17(5):652–660, May 2014.

[52] C. J. Stam. Modern network science of neurological disorders. *Nature Reviews Neuroscience*, 15(10):683–695, Oct. 2014.

[53] K. Supekar, V. Menon, D. Rubin, M. Musen, and M. D. Greicius. Network analysis of intrinsic functional brain connectivity in alzheimer's disease. *PLoS Computational Biology*, 4(6), June 2008. PMID: 18584043 PMCID: PMC2435273.

[54] M. Tschernegg, J. S. Crone, T. Eigenberger, P. Schwartenbeck, M. Fauth-Buhler, T. LemÃĺnager, K. Mann, N. Thon, F. M. Wurst, and

M. Kronbichler. Abnormalities of functional brain networks in pathological gambling: a graph-theoretical approach. *Frontiers in Human Neuroscience*, 7, Sept. 2013.

[55] N. Tzourio-Mazoyer, B. Landeau, D. Papathanassiou, F. Crivello, O. Etard, N. Delcroix, B. Mazoyer, and M. Joliot. Automated anatomical labeling of activations in SPM using a macroscopic anatomical parcellation of the MNI MRI single-subject brain. *NeuroImage*, 15(1):273–289, Jan. 2002.

[56] S. Vergun, A. S. Deshpande, T. B. Meier, J. Song, D. L. Tudorascu, V. A. Nair, V. Singh, B. B. Biswal, M. E. Meyerand, R. M. Birn, and V. Prabhakaran. Characterizing Functional Connectivity Differences in Aging Adults using Machine Learning on Resting State fMRI Data. *Frontiers in Computational Neuroscience*, 7:38, 2013.

[57] J. L. Vincent, I. Kahn, A. Z. Snyder, M. E. Raichle, and R. L. Buckner. Evidence for a frontoparietal control system revealed by intrinsic functional connectivity. *Journal of neurophysiology*, 100(6):3328–3342, Dec. 2008. PMID: 18799601.

[58] J. Wang, X. Zuo, and Y. He. Graph-based network analysis of resting-state functional MRI. *Frontiers in Systems Neuroscience*, 4:16, 2010.

[59] J.-H. Wang, X.-N. Zuo, S. Gohel, M. P. Milham, B. B. Biswal, and Y. He. Graph Theoretical Analysis of Functional Brain Networks: Test-Retest Evaluation on Short- and Long-Term Resting-State Functional MRI Data. *PLoS ONE*, 6(7):e21976, July 2011.

[60] D. Watts and S. Strogatz. Collective dynamics of 'small-world' networks. *Nature*, 393:244–442, 1998.

[61] S. Whitfield-Gabrieli and J. M. Ford. Default mode network activity and connectivity in psychopathology. *Annual Review of Clinical Psychology*, 8:49–76, 2012.

[62] Q. Yu, J. Sui, S. Rachakonda, H. He, W. Gruner, G. Pearlson, K. A. Kiehl, and V. D. Calhoun. Altered Topological Properties of Functional Network Connectivity in Schizophrenia during Resting State: A Small-World Brain Network Study. *PLoS ONE*, 6(9):e25423, Sept. 2011.

[63] W. Yuan, S. L. Wade, and L. Babcock. Structural connectivity abnormality in children with acute mild traumatic brain injury using graph theoretical analysis. *Human Brain Mapping*, 36(2):779–792, Feb. 2015.

[64] Z. Zhang, W. Liao, H. Chen, D. Mantini, J.-R. Ding, Q. Xu, Z. Wang, C. Yuan, G. Chen, Q. Jiao, and G. Lu. Altered functionalâĂŞstructural coupling of large-scale brain networks in idiopathic generalized epilepsy. *Brain*, 134(10):2912–2928, Oct. 2011.

Figure 5: Connectivity network for target network removal in both conditions.

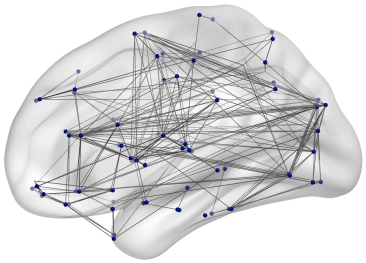

(a) DMN lesioning in young

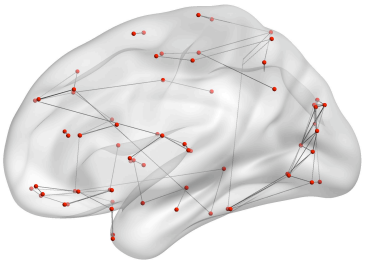

(b) DMN lesioning in elderly

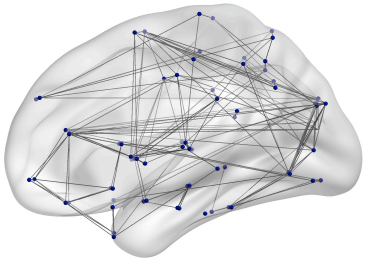

(c) Frontal lesioning in young

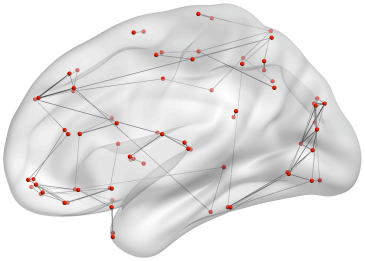

(d) Limbic lesioning in elderly

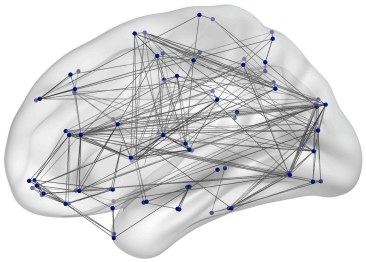

(e) Central lesioning in young

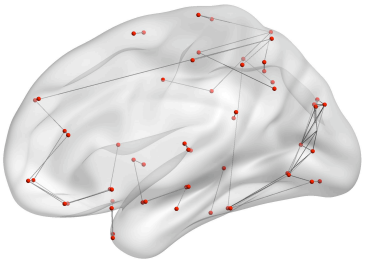

(f) Frontal lesioning in elderly

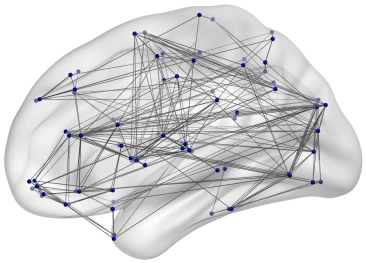

(g) Limbic lesioning in young

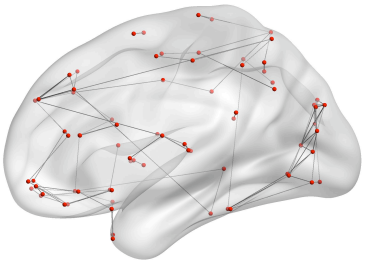

(h) Limbic lesioning in elderly